INTERNATIONAL JOURNAL OF LATEST TECHNOLOGY IN ENGINEERING, MANAGEMENT & APPLIED SCIENCE (IJLTEMAS)

ISSN 2278-2540 | DOI: 10.51583/IJLTEMAS | Volume XIV, Issue VII, July 2025

Solar Irradiance Measurement and Optical Depth Computation Based on Date Time and Latitude, Using A Locally Developed Python Algorithm

Idemudia Godwin[1], Godwin Alexander[2]

[1]Department of Pure and Applied Physics, Federal University Wukari, Nigeria.

[2]Department of Computer Science, Federal University Wukari, Nigeria.

DOI: https://doi.org/10.51583/IJLTEMAS.2025.1407000113

Received: 17 July 2025; Accepted: 21 July 2025; Published: 18 August 2025

Abstract - A locally developed python programming language algorithm was used in the deduction of optical depth (OD) for solar irradiance measurement at 500nm, 675nm and 875nm solar wavelengths at Ilorin (Long. 8.573°N, Lat. 4.5444°E) Nigeria. Results obtained indicate a positive trend in all three wavelength measurements in January of 2003, 2013, and 2024. The correlation with report of desert encroachment which was measured as about 0-6km per year indicates clearly that OD measurement can be used as a precursor to desert encroachment. Results of measurements made in November, December and January of 2003/2004, 2013/2014 and 2024/2025 give a positive trend in both parameters especially at the 500nm and 675nm wavelengths. Hence the result is quite encouraging being the first of such comparison at the sub-Saharan site.

Keywords – Optical Depth, Algorithm, Eko MS120, Sun Photometer, Desertification, Harmattan

I. Introduction

The need for global scale information on surface climate parameters has led to the development of surface methods to retrieve such information from measurements of existing irradiance at the top of the atmosphere (TOA) and a prior information on the atmospheric state, e.g. water vapour, aerosols and ozone. Least is known on the temporal and spatial variation of atmospheric aerosols, in particular, about their optical thicknesses. Recently attempts have been made to derive aerosol optical thickness over oceans from the visible channels of the Advanced Very High-Resolution Radiometer (AVHRR) on board the NOAA operational satellites [1]-[2]. In both cases, long term ground observations were made to validate the satellite interference techniques.

The objective of this work was to obtain information on the variability of aerosol optical thickness in a region of sub-Saharan Africa known to be under the influence of the dusty Harmattan wind and to use this information in subsequent studies to assess downward (SW↓) radiation from satellite observations. To what extent heavy dust loading alter the surface energy budget is currently the object of intense research. In this report, result of irradiance measurement have been computed with a self-designed python algorithm to compute the OD at 500nm, 675nm, and 874nm solar irradiance. The fact that such dust can have an effect far from its origin has been previously documented [3]. Optical depth measurements have shown positive signs in climate studies relating desertification control.

The first and second channels of this instrument are situated in the visible part of the solar spectrum making them suitable for aerosols and desertification studies, which is a product of climate change. Human activities amongst other factors lead to reduced plant cover, exposing the soil to direct sunlight and excessive evaporation. This phenomenon in arid locations have been previously studied by [4] and the report indicated a 0.6km yearly southwardly expansion into sub-Sahara Africa. It is also observed in their work that the three months of November, December and January are periods where the expansion mainly occurs.

Results of aerosol studies by [5]-[6] show a positive increase in OD in the aforementioned months particularly at the solar visible channels. The correlation between desert encroachment data and aerosol OD variation is first, in recent literature, to be studied in the Ilorin observatory.

II. Methodology, the Site, Instrument Specifications and Calibration

Measurements of spectral intensity were made at Ilorin, Nigeria (08°32'N; 04°34'E) in the Harmattan months of 2024 under a TETfund sponsored research. According to [7] Nigeria can be divided into four climatic zones of about 2° latitudinal width. The uppermost part of the Sahelian Zone followed by the Midland area, the Guinea Savannah zone and the Coastal area. Ilorin (located at the upper tip of the Guinea Savannah zone) experiences alternating and thematic southward and northward passages of the Inter-Tropical Convergence Zone (ITCZ). During the dry season (November-February) when the ITCZ appears at slightly south or north of Ilorin the prevailing north easterly wind known as HARMATTAN brings Saharan dry and dust laden air. The dust plumes originate from the Bodele Depression in the Chad basin [8]. During the "wet" season (March-October) conditions are typified by moist maritime south-westerly flow from the Gulf of Guinea over West Africa.

Part of this work is to measure the relative irradiance of the directly transmitted solar radiation at half hourly intervals when the solar disc was clear of clouds using and Eko Sun photometer MS120 described by [9]. Data have been collected in Ilorin between

ISSN 2278-2540 | DOI: 10.51583/IJLTEMAS | Volume XIV, Issue VII, July 2025

November 2024 to January 2025. During the period, three of the four filters whose wavelengths are centred at 500, 675 and 875nm were in continuous use with storage in a data logger. OD results will be presented for these three of the four wavelengths in the instrument. [10] has discussed error terms involved in precision and photometry. These error terms include instrumental errors, calibration errors and errors imposed by the atmosphere (table 2). Based on that study, it could be concluded that uncertainties brought about by diffused radiation within the field of view of the sun photometer, in this case, 2.4° are negligible for the wavelengths and OD. The total OD of the atmosphere was determined by making a fit of the Lambert-Beer law given by;

$I(\lambda) = \gamma I_o(\lambda) \exp(\zeta(\lambda)\, m(\theta))$ ……..1

Where $I(\lambda)$ is solar irradiance reaching the detector at wavelength λ, $I_o(\lambda)$ is the calibration equivalent of the irradiance at the top of the atmosphere (Fig. 1), $m(\theta)$ the atmospheric airmass which is a function of the solar zenith angle θ_o and $\zeta(\lambda)$ is the OD and γ is the variable Sun-Earth distance correction.

Table 1 Calibration Parameters for EKO 120 Compared to World Meteorological Standard [10]

Specification	Eko 120	WMO
Full view angle (°)	2.4	2.4
Linearity (% of full scale)	±0.2	±0.2
Precision (% of full scale)	0.2	0.1
Stability (% of full scale)	±0.2	±0.1
Half band width (nm)	0.6	0.5
Normal wavelength (nm)	500	500
	675	775
	875	844

The Eko sun photometer model SM120 manufactured by the Eko instruments trading company ltd, Japan used in this study has a quartz window that is well blocked and thin-film interference filters with peak wavelengths accuracy to ±2nm and half band width 20-40% window and the filters are 5 nm in radius

$V_o(\lambda,T)$ is the voltage output corresponding to irradiance at zero airmass, mean Sun-Earth distance and 25°C ambient temperatures. α is the temperature coefficient by which output voltage $V(\lambda,T)$ is corrected and T is the measured temperature in °C

$V_o(\lambda, T=25°C) = V[\lambda , T\{1-\alpha (T-25°C)\}]$…….2

A similar instrument was used by [9] during the 1990 dust storm in Maiduguri (Lat 11.8311°N, Long 13.1510°E)

The calibration values of the instruments exoterrestrial solar flux is compared to the WMO standard in table 1

B. Procedures to Derive Optical Depth

The expression used to determine the aerosol optical thickness is the Lambert-Bouguer-Beer Law given by:

$V(\lambda) = V_0(\lambda)\varepsilon \exp[(-m_a \tau_a + m_r \tau_r + m_z \tau_z)]$ ……..3

where $V(\lambda)$ is the solar irradiance which reaches the detector at wavelength λ; $V_0(\lambda)$ is the extraterrestrial solar irradiance; $\varepsilon = (r_m / r)^2$ where r_m is the mean Earth-Sun distance and r is the actual Earth-Sun distance; τ_a, τ_r and τ_z are the aerosol, Rayleigh and ozone ODs; and m_a, m_r and m_z are the corresponding airmasses along the path to the sun. Separate airmass terms are used for each constituent because they are concentrated at different heights within the atmosphere. The following expression was used to compute the Rayleigh air mass [11]:

$m(\theta_o) = (\cos \theta_o + 0.025 \exp(-11 \cos \theta_o))^{-1}$ …...….4

where θ_o is the solar zenith angle. The solar zenith angles were computed using the equations of the Greenwich hour angle and solar declination given for each month in the [12] for the appropriate year of measurements. The aerosol air mass was derived assuming that the aerosols are concentrated in the lowest 2 km while the ozone air mass was derived assuming that ozone is concentrated at heights between 15 and 20 km from the Earth's surface.

Three of the wavelengths of the EKO sun photometer used in this study (500, 675, 875 nm) lie in the window regions where the average absorption (excluding ozone and NO_2) is less than 0.3% [13]. The fourth wavelength (945 nm) lies in a water vapor absorption band. Results based on observations in the window regions only, is being presented. The annual variation of ozone concentration as appropriate for each latitude was accounted for, using climatological values as reported in [14].

ISSN 2278-2540 | DOI: 10.51583/IJLTEMAS | Volume XIV, Issue VII, July 2025

The Rayleigh optical thickness was computed using:

$\tau_r = (P/P_0)\,[0.008569\lambda^{-4}\,(1 + 0.0113\lambda^{-2} + 0.00013\lambda^{-4})]$…….5

where P_0 = 1013 mb and λ is in µm, as given by [15].

The diffuse flux entering the instrument's 2.4° field of view is not included in Eq. (1) since the amount of diffuse radiation entering the instrument is less than 2% for solar zenith angles less than 80° and ODs less than 2 [16]-[17].

In this study, only data collected during the 2024/2025 Harmattan season will be used. The aerosol optical depth was computed, using interpolated zero airmass voltages from the calibration curves, as appropriate for each observation period. Such analysis is possible only in retrospect.

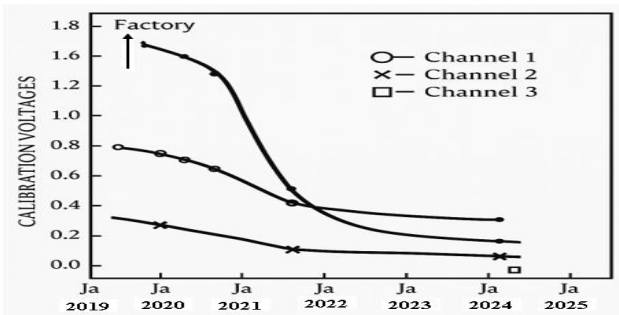

Fig. 1: Calibration drift of the EKO Model SM-120 photometer used in this study

Table 2: Error Analysis of the measurement Data at Ilorin Airport at Solar noon

Date [(Local time in 2024/2025) (12hr 34min: 4sec)]

Date	Time	$d\check{c}/dP$ Optical thickness at 500nm	$d\theta/dP$ Elterman's Vertical	$\frac{d\check{c}}{dP} - \frac{d\theta}{dP}$
22 Nov	09:00 – 13:00	0.8112	0.4513	-
27 Nov	09:00 – 13:00	0.7522	0.4916	0.17
06 Dec	09:00 – 13:00	1.0251	0.9241	0.08
10 Dec	09:00 – 13:00	1.1230	0.9932	0.09
05 Jan.	09:00 – 13:00	0.7521	0.7035	0.019
10 Jan.	09:00 – 13:00	0.6901	0.6423	0.0400
01 Feb.	09:00 – 13:00	0.2030	0.1131	0.0600
15 Feb.	09:00 – 13:00	0.2000	0.1015	0.0300
Mean Standard Error:		0.6946 ± 0.0210	0.5526 ± 0.0223	0.06986 ± 0.0013

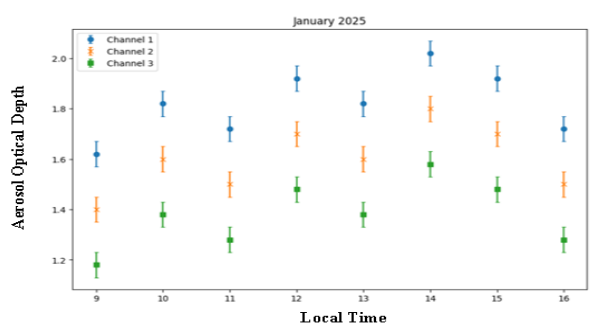

Fig. 2: Monthly mean diurnal variation of aerosol optical depth at Ilorin, Nigeria (Dec. 19, 2024)

ISSN 2278-2540 | DOI: 10.51583/IJLTEMAS | Volume XIV, Issue VII, July 2025

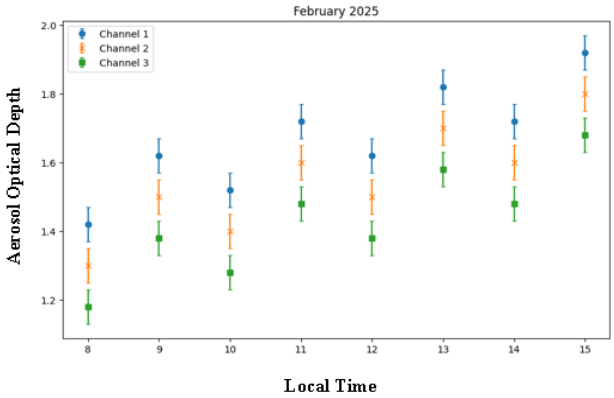

Fig. 3: Monthly mean diurnal variation of aerosol optical depth at Ilorin, Nigeria (Jan. 10, 2025)

III. Results

Diurnal Variation of Optical Depth for Selected Similar Days of Three-Year Data: In Fig. 2 and 3, we present the diurnal variation of the spectral aerosol optical depth at Ilorin, Nigeria for December 19, 2024 (Fig.2) and for January 10, 2025 (Fig. 3). The observations were taken at half hourly intervals, and repeated about 3-5 times for each case to enable the detection of invisible cirrus clouds. For the characteristic cases shown, the aerosol optical depth at 500 nm was above 0.8; highest values of 1.6-1.8 were reached on January 10, 2025, which was reported to be a day of a very dense dust. The values were relatively stable with little diurnal variability; on December 19, 2024 a steady increase in the aerosol optical depth during the day reached a maximum in late afternoon; on January 10, 2025, maximum was reached around noon [Fig.3]. These distinct patterns could have been related to diurnal wind effects which could have brought in more dust laden air.

During December of 2024, the aerosol optical depth was remarkably stable at about 1.1 at 500 nm. During January of 2025 all channels peak were as high as 1.0 at 500 nm around noon. In February '25, the behavior was less systematic, possibly due to fewer observations.

In Fig. 4 we present an example of the monthly mean diurnal variation for December 2023 [5]. The patterns are similar to those of 2024 and the aerosol optical depths at 500 nm are above 1.0, however, the aerosol optical depth in channel 2 exceeded somewhat the one in channel 1. Similar event occurred in December 2013 [6]

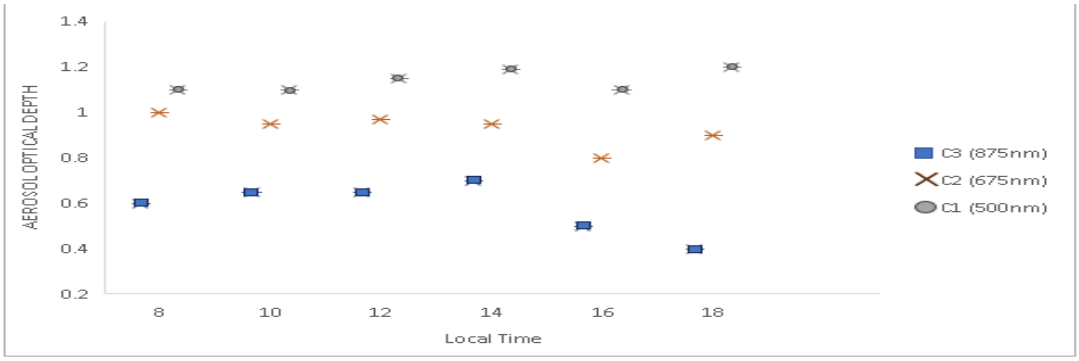

Fig. 4: Diurnal Variation of Optical Depth measurement in December 2003 [5]

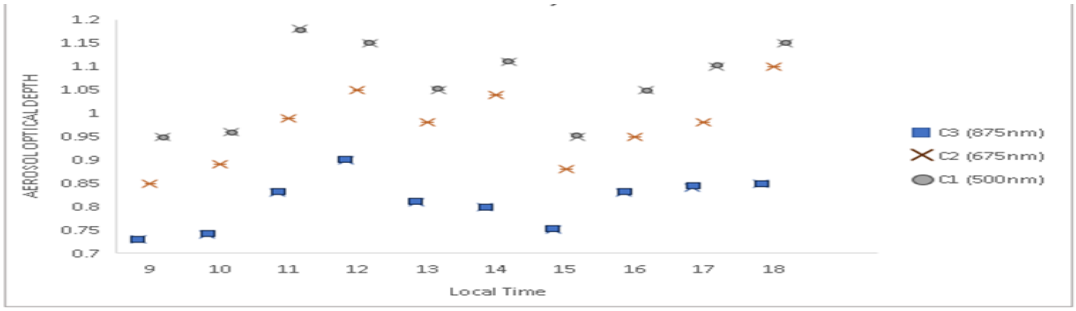

Fig. 5: Diurnal Variation of Optical Depth measurement in December 2013 [6]

ISSN 2278-2540 | DOI: 10.51583/IJLTEMAS | Volume XIV, Issue VII, July 2025

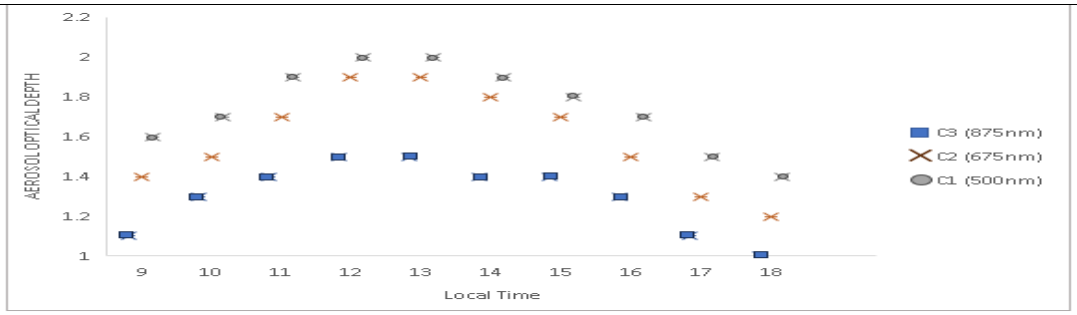

Fig. 6: Diurnal Variation of Optical Depth measurement in December 2024

Table 3: Optical depth computed and Compared for Various Years

Diurnal mean optical depth in December	2003	2013	2024
500nm	1.054	1.135	1.933
675nm	0.851	0.956	1.712
875nm	0.750	0.657	1.401

From the results in Table 3, OD measurements in the visible band responded positively to the trend in desert encroachment over the year 2003, 2013 and 2024 (Fig. 4, 5 and 6). However, this factor may also be influenced by other variables which require further studies. Table 3 shows the consistency of the increase in OD over the years of measurement which is an indication of the trend in OD variation. OD studies, over a longer period of time, can be a precursor to desertification which has a progression rate of 0.6Km per year in the Sahelian region of Nigeria.

IV. Conclusion

The reason for a decrease in the rainfall in the Sahel during the last three decades is yet to be fully understood. Of particular interest are the plausible feedback mechanisms that come into play as a result of an initial decrease in rainfall. Little is known of the possible effect aerosol play in this process as a result of drier surface conditions. The proposal of the possible effect of dust particles in desertification studies has been undertaken by [18] but no study has been made showing how aerosols OD variation predict desert encroachment on real time scale. Therefore, we can, somehow, predict that an increase in aerosol mass loading during the Harmattan season could be a contributory factor in drought intensity in the Sahel.

Dust storms contribute significantly to the inventory of tropospheric aerosols and are part of the natural variability of tropospheric aerosols. In the present study results are presented that indicate that aerosols are precursors to desertification while the algorithm (appendix) used in analyzing this huge data, has been found quite suitable for this studies.

V. Acknowledgement

This work was supported by Institution Based Grant IBR 2021 TETfund Intervention to Tetiary Institutions

References

1. Rao, C. R. N., Stowe, L. L., and McClain, E. P. (2002). Remote sensing of aerosols over oceans using AVHRR data: Theory, practice and applications. International Journal of Remote Sensing, 10, 743–749.
2. Kaufman, Y. J., and Holben, B. N. (2010). Calibration of the AVHRR visible and near-IR bands by atmospheric scattering, ocean glint and desert reflection. International Journal of Remote Sensing, 14(1), 21–52.
3. Carlson, T. N., and Prospero, J. M. (2000). The large-scale movement of Saharan air outbreaks over the northern equatorial Atlantic. Journal of Applied Meteorology, 11, 283–297.
4. Audu I.A. and Adie L.A. (2018). Desertification in Northern Nigeria; J. of Envir. Management: http/cepajournal.com
5. Pinker R.T. (2003) Measurement of Atmospheric Turbidity and Wavelength Exponent in the Saharan Dust Plume., J. of Aerosol society Vol.17(5) Pg 453-462
6. Aro T. O, Idemudia, G. (2013) Characteristic Aerosol Optical Depth in Sub-Saharan Africa. Geophysics Research Letters; VOL23 No.8 Pg 685-688
7. Olaniran, O. J. (1999). Evidence of climatic change in Nigeria based on annual series of rainfall of different daily amounts, 1949–1985. Climatic Change, 19, 319–341
8. Bertrand, J., Cerf, A., and Domergue, J. K. (1979). Repartition in space and time of dust haze south of the Sahara. W. M. D., 538, 409–415.
9. Oluwafemi, C.O. (1991). Particle Size Distribution, Turbidity and Angular Scattering in the Harmattan Regime. Journal of Geophysical Research, Vol. 23, 687-690.

ISSN 2278-2540 | DOI: 10.51583/IJLTEMAS | Volume XIV, Issue VII, July 2025

10. Forgan B.W. (1976). Aerosol Optical Depth at Sea Level Station, CGBAPS Cape Cirim. Technical Report 5
11. Rosenberg, G. V. (1966). Twilight: A study in atmospheric optics (English translation). Plenum Press.
12. Almanac for Weather Computation (2022, 2023, and 2024). Nautical Almanac Office, U.S. Government Printing Office. Washington, DC.
13. King, M. D., Byrne, D. M., Reagan, J. A., and Herman, B. M. (1993). Spectral variation of optical depth at Tucson, Arizona between August 1975 and December 1977. Journal of Applied Meteorology, 19, 723–732.
14. London L.J. (1976). Optical and radiative properties of a desert aerosol model. Unpublished.
15. Hansen, J., and Travis, L. (1974). Light scattering in planetary atmospheres. Space Science Reviews, 16, 527–610
16. Shaw, G. E., Reagan, J. A., and Herman, B. M. (1973). Investigations of atmospheric extinction using direct solar radiation measurements made with a multiple wavelength radiometer. Journal of Applied Meteorology, 11, 374–380.
17. Grassl, H. (1971). Calculated circumsolar radiation as a function of aerosol type, field of view, wavelength, and optical depth. Applied Optics, 10, 2542–2543.
18. McTainsh, G. H. (2022). Harmattan dust deposition in northern Nigeria. Nature, 286, 587–588.

Appendix

Python Programming Algorithm for Computing Optical Thickness Using Measurement Date, Irradiance Data, Time and Latitude

```
import math
# Convert degrees to radians
def deg_to_rad(deg):
    return math.radians(deg)
# Convert radians to degrees
def rad_to_deg(rad):
    return math.degrees(rad)
# Get user input
day = int(input("Enter the day of the year (1–365): "))
Atime = float(input("Enter the time in 24-hour format (e.g., 13.25 for 1:15 PM): "))
latitude = float(input("Enter latitude in degrees (positive for N, negative for S): "))
# Calculate ecliptic longitude of the sun (Lam)
Lam = 360 * (day + 1) / 365
Lam_rad = deg_to_rad(Lam)
# Calculate Equation of Time (Et) in minutes
Et = ( 0.000075 +0.001868 * math.cos(Lam_rad) -0.032077 * math.sin(Lam_rad) -
    0.014615 * math.cos(2 * Lam_rad) - 0.04089 * math.sin(2 * Lam_rad)) * 229.18
# Calculate solar declination (Decl) in radians    3
Decl = ( 0.006918 -0.399912 * math.cos(Lam_rad) + 0.070257 * math.sin(Lam_rad) -
    0.006758 * math.cos(2 * Lam_rad) + 0.000907 * math.sin(2 * Lam_rad) -
    0.002697 * math.cos(3 * Lam_rad) + 0.00148 * math.sin(3 * Lam_rad))
# Adjust input time
Tim = Atime - 1
Xtim = int(Tim)
Ytim = Tim - Xtim
Aztim = Ytim * 60
Ztim = Aztim * 100
Atim = Xtim + Ztim / 100
```

ISSN 2278-2540 | DOI: 10.51583/IJLTEMAS | Volume XIV, Issue VII, July 2025

```
Alat = Atim + 0.30444
# Calculate hour angle (Anghr) in radians
Anghr_deg = (Alat - 12 - Et / 60) * 15
Anghr = deg_to_rad(Anghr_deg)
# Convert latitude to radians
Lat_rad = deg_to_rad(latitude)
# Calculate solar zenith angle cosine using formula:
# cos(Zenith) = sin(lat)*sin(dec) + cos(lat)*cos(dec)*cos(hour angle)
cos_Zen = math.sin(Lat_rad) * math.sin(Decl) + math.cos(Lat_rad) * math.cos(Decl) * math.cos(Anghr)
cos_Zen = max(min(cos_Zen, 1), -1)  # Clamp to [-1, 1] to avoid domain errors
# Calculate Zenith angle in radians
Zenith = math.acos(cos_Zen)
Theta = Zenith  # Zenith angle used as Theta in radians
# Air mass model calculations
Ax = math.cos(Theta)
Theta_deg = rad_to_deg(Theta)
Bx = 0.15 * ((90 - Theta_deg) + 3.885) ** (-1.253)
# Extraterrestrial solar radiation (Es)
Es = ( 1.000110 + 0.034221 * math.cos(Lam_rad) +0.001280 * math.sin(Lam_rad) +
    0.000719 * math.cos(2 * Lam_rad) + 0.000077 * math.sin(2 * Lam_rad))                    4
# Air mass (Amass)
Amass = 1 / (Ax + Bx)
# Measured irradiance (Em)
Em = Amass * 972.75 / 1013.25
# Output results
print("\n--- Solar Position Calculations ---")
print(f"Day of year: {day}")
print(f"Time (decimal hours): {Atime}")
print(f"Latitude: {latitude}°")
print(f"Declination: {rad_to_deg(Decl):.4f}°")
print(f"Equation of Time: {Et:.2f} miSnutes")
print(f"Hour Angle: {Anghr_deg:.2f}°")
print(f"Zenith Angle: {Theta_deg:.2f}°")
print(f"Extraterrestrial Radiation (Es): {Es:.4f}")
print(f"Air Mass (Amass): {Amass:.4f}")
print(f"Estimated Irradiance (Em): {Em:.4f} units") {Fig. 1 and 2]
```